Journal of Power Sources 184 (2008) 420–426

Contents lists available at ScienceDirect

Journal of Power Sources

journal homepage: www.elsevier.com/locate/jpowsour

PVDF-HFP-based porous polymer electrolyte membranes for lithium-ion batteries

Ruiying Miao [a], Bowen Liu [a], Zhongzheng Zhu [a], Yun Liu [a], Jianling Li [a], Xindong Wang [a,*], Qingfeng Li [b]

[a] Department of Physical Chemistry, University of Science and Technology Beijing, Beijing 100083, China
[b] Department of Chemistry, Technology University of Denmark, DK-2800 Lyngby, Denmark

ARTICLE INFO

Article history:
Received 4 January 2008
Received in revised form 5 March 2008
Accepted 18 March 2008
Available online 26 March 2008

Keywords:
Electrolyte
Lithium-ion battery
Porous
Polymer membrane

ABSTRACT

As a potential electrolyte for lithium-ion batteries, a porous polymer electrolyte membrane based on poly(vinylidenefluoride-hexafluoropropylene) (PVDF-HFP) was prepared by a phase inversion method. The casting solution, effects of the solvent and non-solvent and addition of micron scale TiO_2 particles were investigated. The membranes were characterized by SEM, XRD, AC impedance, and charge/discharge tests. By using acetone as the solvent and water as the non-solvent, the prepared membranes showed good ability to absorb and retain the lithium ion containing electrolyte. Addition of micron TiO_2 particles to the polymer electrolyte was found to enhance the tensile strength, electrolyte uptake, ion conductivity and the electrolyte/electrode interfacial stability of the membrane.

1. Introduction

Since the ionic conductivity was discovered in complexes of poly(ethylene oxide) (PEO) containing alkali metal salts in 1970s [1,2], solid polymer electrolytes (SPEs) have received much attention [3]. Compared with other types of electrolytes, SPEs have advantages of being mechanically elastic, low in weight, easy to handle, and therefore have potential applications in electrochemical devices such as high energy batteries, electrochromic display devices, chemical sensors and polymer electrolyte fuel cells.

For uses in high energy batteries, there are three types of SPEs according to the structure patterns: namely dry solid polymer electrolyte (DSPE), gel solid polymer electrolyte (GSPE), and porous solid polymer electrolyte (PSPE). A variety of polymers with different chemical structures, ranging from PEO, poly(vinylidene fluoride) (PVDF) and its copolymers, poly(methyl acrylate) (PMMA) to poly(vinyl chloride) (PVC), have been employed as matrix materials for SPEs [4–10].

Among these, PVDF and its copolymers used as matrix for PSPE have been extensively studied because of its high solubility, the lower crystallinity and lower glass transition temperature [11,12]. The PSPE, however, have poor mechanical properties, thermal and interfacial instability [13,14]. One way to improve properties of the PSPE is to add inorganic fillers, such as SiO_2, TiO_2, Al_2O_3, and Sm_2O_3, in the polymer electrolyte [14–21]. Usually, these inorganic fillers are dispersed in the polymer electrolyte in the form of nanoparticles, however, nanoparticles tend to aggregate because of the high surface energy. For example, Kim et al. [22] reported that TiO_2 nanoparticles cannot be well dispersed, even under conditions such as ultrasonication and the subsequent ball-milling.

In this study, the (PVDF-HFP)-based PSPE was prepared by the phase inversion method. The preparation process of the casting solution and effects of solvent and non-solvent on the configuration and performance have been investigated. The influence of micron particles of TiO_2 incorporated in PSPE on the structure and properties of PSPE have been examined.

2. Experimental

2.1. Preparation of the electrolyte membrane

The PVDF-HFP (Kynar^{TM} 2801, Elf Atochem) was dissolved in a mixture of a solvent and a non-solvent (the ratio of solvent and polymer is 9–12, and the ratio of non-solvent and polymer is 0.25–0.5). The dissolution took place at 50–60 °C for about 2 h under continuous stirring. The solvents were typically selected from acetone, tetrahydrofuran, *N*-methyl pyrrolidone (NMP) and others. The non-solvents can be water, ethanol, butanol, etc.

* Corresponding author. Tel.: +86 10 62332651; fax: +86 10 62332265.
E-mail addresses: echem@ustb.edu.cn (X. Wang), lqf@kemi.dtu.dk (Q. Li).

0378-7753/$ – see front matter © 2008 Elsevier B.V. All rights reserved.
doi:10.1016/j.jpowsour.2008.03.045

A transparent and viscous solution containing 5–10% PVDF-HFP was obtained. For preparing the composite PSPE, an appropriate quantity of TiO_2 micron particles (D_{50} = 1.4 μm, C.R., Tianjin) was dispersed in the PVDF-HFP solution with help of an ultrasonic crasher. The solution was then cast onto a glass plate by a doctor blade. A white porous membrane was obtained after the evaporation of the volatile solvent and non-solvent at room temperature. Generally, the thickness of the porous membrane is about 50 μm.

The dry porous membrane was then immersed in a lithium-ion battery electrolyte solution under dry argon atmosphere in a glove box (MECAPLEX, CH-2540, Grenchen, Switzerland). The solution consists of 1 mol L^{-1} $LiPF_6$ in a mixture of ethylene carbonate (EC) and dimethyl carbonate (DMC) in a weight ratio of 1:1. Thus, obtained membrane was ready for electrochemical performance measurements.

2.2. Characterization of physical properties

The porosity of the porous membrane was calculated by the following equation:

$$\rho = \frac{\Delta V_{\text{water}} - \Delta V_{\text{ethanol}}}{\Delta V_{\text{water}}} \times 100\% \quad (1)$$

where ΔV_{water} is the increased volume of the de-ionized water before and after the dry membrane being immersed in and $\Delta V_{\text{ethanol}}$ is the increased volume of the ethanol.

A piece of the dry porous membrane was immersed in the lithium ion electrolyte solution for at least 2 h at room temperature. Then the membrane was taken out of the solution, gently blotted with paper tissue. The membrane was weighed before and after inhaling the electrolyte solution. The electrolyte uptake of the porous membrane was calculated by the following equation:

$$\theta = \frac{W_{\text{wet}} - W_{\text{dry}}}{W_{\text{dry}}} \times 100\% \quad (2)$$

where W_{wet} is the weight of the wet membrane, and W_{dry} is the weight of the dry membrane.

The tensile stress of the membranes was measured using a Letry Tensile Tester. The test specimens were prepared as the standard method. The tensile rate is 1 mm min^{-1}. The tensile strength, T, was calculated by the following equation:

$$T = \frac{P}{S} \quad (3)$$

where P is the tensile force at break applied on the sample, S is the cross-section area of the sample. In practice, the real area of the sample during stretching cannot be measured. Here the S is the initial cross-section area and the T is therefore the engineering stress.

The surface morphology of the porous membrane was examined by a Cambridge S-360 scanning electron microscope (SEM). X-ray diffraction (XRD) patterns were recorded with an X-ray diffractometer (MAC MXP21VAHF) by using monochromatic Cu Kα radiation.

2.3. Electrochemical characterization

In a glove box filled with pure argon, a disk of the electrolyte membrane (A = 0.5 cm^2) was sandwiched between two Ni electrodes to assemble a Ni/electrolyte/Ni blocking closed cell. The ionic conductivity of the polymer electrolyte was measured by impedance spectroscopy at room temperature, over the frequency range from 300 kHz to ~10 Hz with an AC size wave amplitude of 20 mV. The ionic conductivity was measured in a temperature range of 30–80 °C. Before each measurement, the cell was left for half an hour to reach a thermal equilibrium. The ionic conductivity (σ) was calculated from the bulk resistance (R) using the relation $\sigma = L/(R \times A)$, where L and A represent the thickness and the area of polymer electrolyte film, respectively.

The anodic break-down voltage was evaluated by running current–voltage sweeps on two-electrode cells using a Ni working electrode, a lithium counter electrode and the membrane sample as the electrolyte. Under these conditions, the onset of current was assumed to indicate the decomposition voltage of the electrolyte. The interfacial stability between the polymer electrolyte and the lithium metal electrode was evaluated by impedance response of symmetric Li/electrolyte/Li cells. The cells were stored under open circuit conditions at room temperature. All the electrochemical experiments were carried out using a VMP2 multichannel potentiostat (Princeton Applied Research).

To evaluate the rate capability of the lithium-ion battery using this polymer electrolyte as the separator, we assembled a $LiCoO_2$/polymer electrolyte/Li model cell. The cathode was prepared from the slurry containing $LiCoO_2$, acetylene black, PVDF-HFP and NMP, with an aluminum substrate. The viscous slurry was spread on the aluminum foil. Then they were dried at high temperature and rolled into electrode film. The thickness of the film was about 230 μm. The film was clipped into small wafers (Ø 8 mm). One of the wafers was assembled as separator of the model cell, $LiCoO_2$ as the cathode, and the lithium metal as anode. The tests were run by using a (Neware) BTS-5 V/10 mA high precision Battery Test System.

3. Result and discussion

3.1. The effect of solvent and non-solvent

During the film-casting process, mutual diffusion promptly occurs between solvent and non-solvent to make highly porous structure in polymer matrix. In other words, two kinds of diffusion with opposite directions are competing in that the solvent component is going to evaporate (or escape) from the spread slurry while the non-solvent to penetrate into (or solidify) it. This method is very beneficial in obtaining planned morphology by controlling preparation conditions such as the kind of solvent and non-solvent, their

Table 1
Effects of solvent and non-solvent on the performance of membrane

Samples	Solvent	Non-solvent	Initial uptake (%)[a]	Retention after 8 days (%)[a]	Weight loss after 8 days (%)[a]	Porosity (%)	Mechanical performance
a	Acetone	Ethanol	76	72	5	13	Stretch-resisting
b	THF	Water	216	200	7	62	Little-brittle
c	THF	Ethanol	42	40	5	10	Stretch-resisting
d	Acetone	Water	297	282	5	75	Little-brittle
e	NMP + acetone	–	288	245	15	87	Brittle
f	NMP + acetone	Water	243	238	5	56	Little-brittle
g	NMP + acetone	Ethanol	210	206	2	50	Little-brittle

[a] Mass percentage.

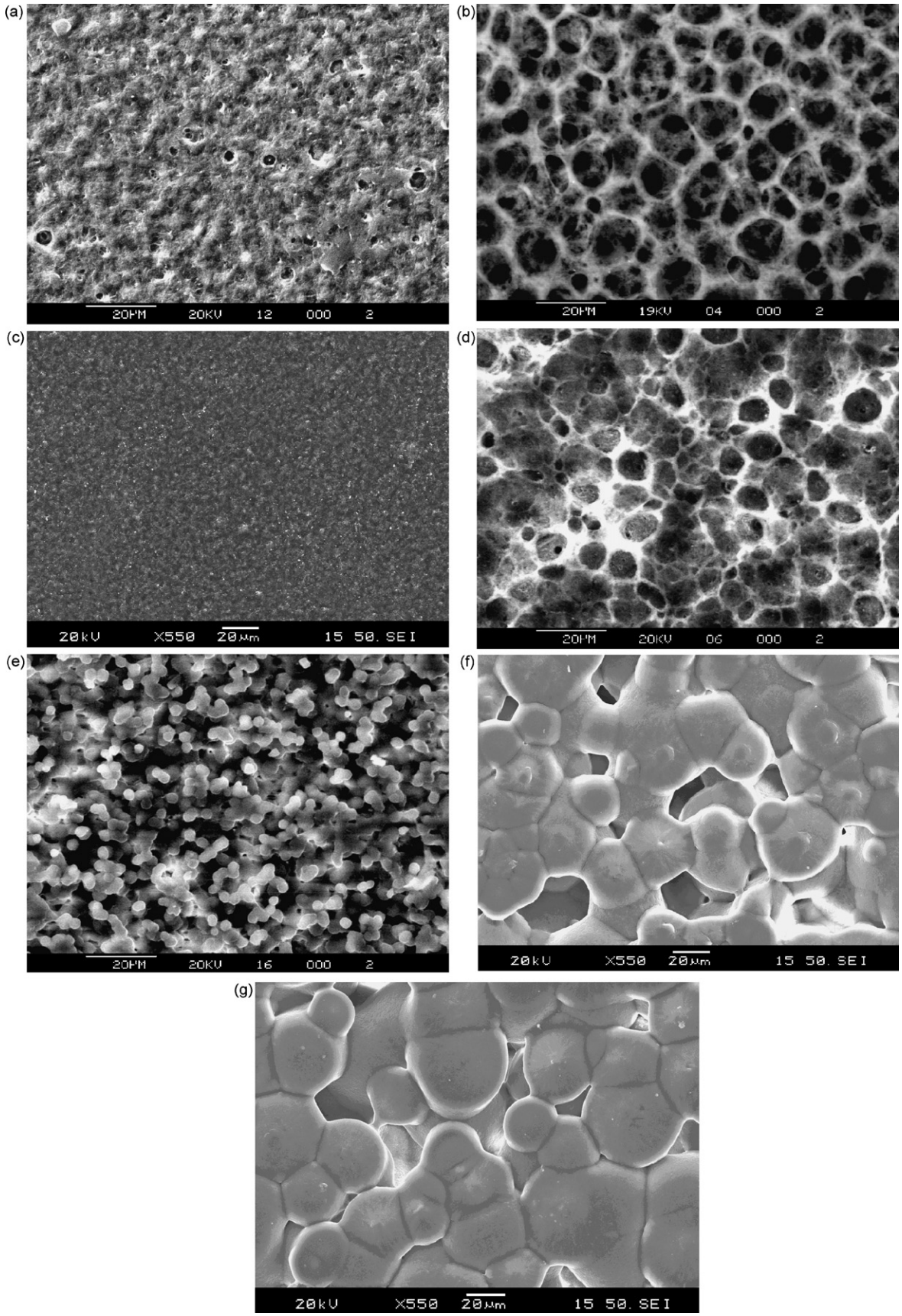

Fig. 1. SEM micrographs of prepared membrane samples. (a) Acetone + ethanol; (b) THF + water; (c) THF + ethanol; (d) acetone + water; (e) NMP + acetone; (f) NMP + acetone + water; (g) NMP + acetone + ethanol.

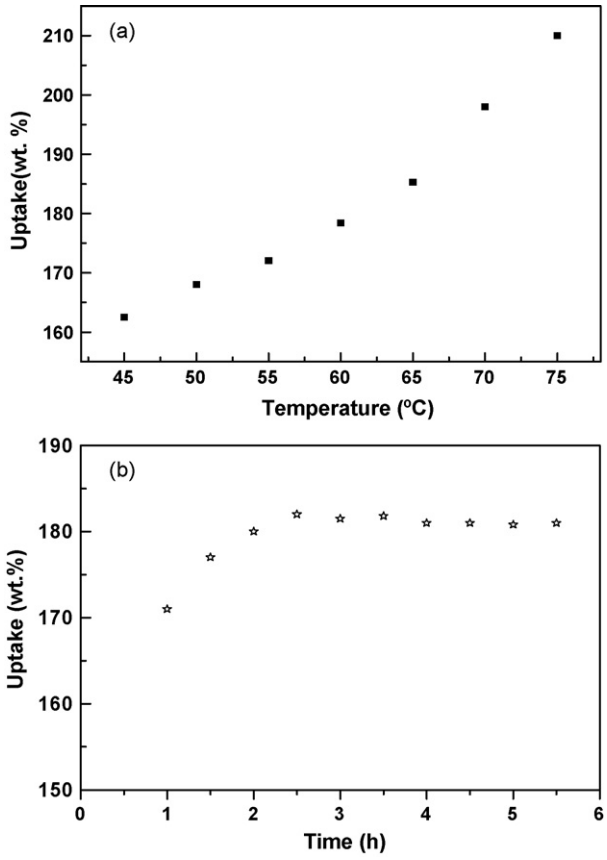

Fig. 2. Effects of preparation technique on performance of membrane. (a) Relationship between uptake of membranes and dissolution temperature; (b) relationship between uptake of membranes and stirring time.

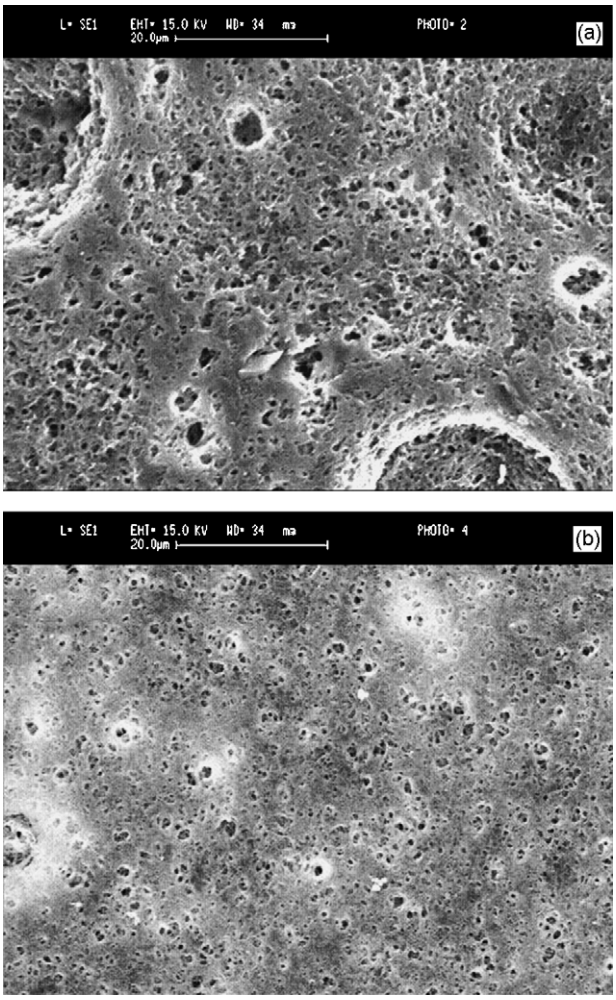

Fig. 3. SEM images of PVDF-HFP polymer films: (a) without TiO_2; (b) with 6.5% TiO_2.

concentration and even the crystallinity of polymer matrix [23]. Several common solvents and non-solvents have been selected for the preparation of the membrane. The used solvents, non-solvents and properties of the resultant porous membranes prepared are summarized in Table 1.

As seen from the table, when the same solvent (acetone in experiments a and d) and different non-solvents (ethanol and water) were used, there is about a fourfold discrepancy of the uptake between the two kinds of membranes. The mechanical property was better when ethanol was used as the non-solvent. On the other hand, the uptake and mechanical property were better when the same non-solvent (e.g. water) but different solvent (THF, acetone and NMP + acetone) were used in experiments b, d and f. In the experiment a and c, the mechanical property was good but the ability of uptake was poor. In the experiment e, the mechanical property of the membranes was not as good as that of the membranes (f and g) prepared with non-solvent.

SEM photos of these membrane samples are shown in Fig. 1. The membranes prepared by the phase inversion method had reticular porous fabric. The membranes prepared THF or acetone as the solvent and water as the non-solvent had higher porosity and the suitable pore size (about 7–15 μm in Fig. 1(b) and 5–10 μm in Fig. 1(d)). These membranes had better ability to retain electrolyte, i.e. with higher electrolyte uptake, other than sample e. On the contrary, those membranes with low porosity and small pore size exhibited lower electrolyte absorption ability. In experiment c (Fig. 1(c)), the low electrolyte absorption ability was because of the compact structure. In experiment e (Fig. 1(e)), only solvent was added, and the resultant membrane seemed to have an irregular reticular porous microstructure. From Fig. 1(f) and (g), we could see the porous structure; but the distribution of the pore and the pore size was irregular. It seems that the solvent and non-solvent chemistry have significant effects on the pore structures and membrane performances. It tends to form porous structure and the pore size is larger when we select water as non-solvent. If the non-solvent is ethanol, the structure of membrane tends to be compact. In the rest of this study, acetone as the solvent and water as the non-solvent are used.

3.2. Factors of the membrane preparation

During the whole process of membrane preparation, dissolution temperature and stirring time are two important factors.

Table 2
Properties of polymer electrolyte membranes with and without TiO_2

No.	TiO_2 mass percentage (%)	Tensile strength (MPa)	Porosity (%)	Uptake (%)	Conductivity ($S\,cm^{-1}$) (25 °C)
1	0	1.53	78.1	320.7	3.36×10^{-4}
2	6.5	2.78	60.0	358.6	1.66×10^{-3}

It is found that polymer dissolution rate is slow at low temperature, and it increases with the increasing of the temperature. By using the elevated dissolution temperature, the obtained porous polymer membrane shows higher electrolyte uptake, as shown in Fig. 2(a), the uptake increases steadily with the dissolution temperature, slightly faster at temperatures above 60 °C. One of the main reasons is that the higher temperature restrains the growth of PVDF-HFP crystallines and is easier to achieve higher uptake. As the solvent and non-solvent are volatile, the evaporation rate accelerates promptly at higher temperatures. In the following study the dissolution temperature we have to choose is 50–60 °C.

The influence of the stirring time on the electrolyte uptake of the obtained porous polymer membrane is depicted in Fig. 2(b). Generally, the polymer could not be dissolved thoroughly within a short time. In practice, it was observed that the polymer dissolved completely about 2 h at 50–60 °C, when a transparent polymer solution was obtained. After that any longer stirring time did not seem to further improve the membrane uptake.

3.3. Effects of TiO_2 micron particles

The physical and electrochemical properties of the PVDF-HFP-based polymer electrolyte without and with TiO_2 micron particles have been investigated in this section, the results are shown in Table 2. From the table we can see that the tensile strength, electrolyte uptake and ionic conductivity of the polymer electrolyte membrane were all improved due to the addition of 6.5% TiO_2. The tensile strength increased to 182%. Although the porosity was decreased from 78 to 60%, the electrolyte uptake was however slightly from 320 to 358%. The reason is that TiO_2 particles fill in part of the cavities. But the addition of TiO_2 particles decreases the crystallinity of the polymer and helps the absorption and the keeping of the electrolyte. A fivefold increase in the ionic conductivity was measured.

Fig. 3 shows SEM photographs of the porous membranes. As can be seen from Fig. 3(a), the different size of pores coexisted in the membrane, and the distribution of the pores was not uniform. When TiO_2 was added, the pore size was smaller (less than 2 μm) and the distribution of the pores was uniform, as shown in Fig. 3(b). The membrane doped with TiO_2 had a denser reticular fabric, which improved the mechanical property as well.

The XRD patterns for the membranes are shown in Fig. 4. There are two intense peaks at 18.14° and 19.64° for the pure PVDF-HFP powder (Fig. 4(b)), and obvious differences can be observed when the powder was made of porous membrane (Fig. 4(c) and (e)), a broad peak (①) and aculeate peaks (② , ③ and ⑤) can be observed. The broad peak (①) disappeared and the intensity of aculeate peaks (② , ③ and ⑤) weakened (Fig. 4(d) and (f)) when the porous membranes absorbed electrolyte, which indicated that both the crystallinity and the size of crystal decreased, and so the migration of the polymer chain could be freer. The intensity of peaks (② , ③) decreased relatively, and the intensity of peak (⑤) decreased obviously when a small quantity of TiO_2 added. All these observations indicate that the crystallinity of polymer decreased obviously, which leads to the improvement of ionic conductivity of the polymer electrolyte, to be discussed in the following section.

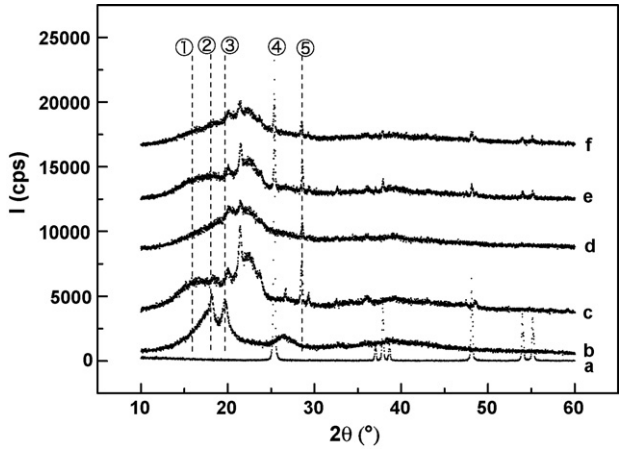

Fig. 4. X-ray diffraction spectra of (a) TiO_2; (b) PVDF-HFP powder; (c) PVDF-HFP-based porous film; (d) PVDF-HFP-based electrolyte; (e) PVDF-HFP-based porous film with TiO_2; (f) PVDF-HFP-based electrolyte with TiO_2.

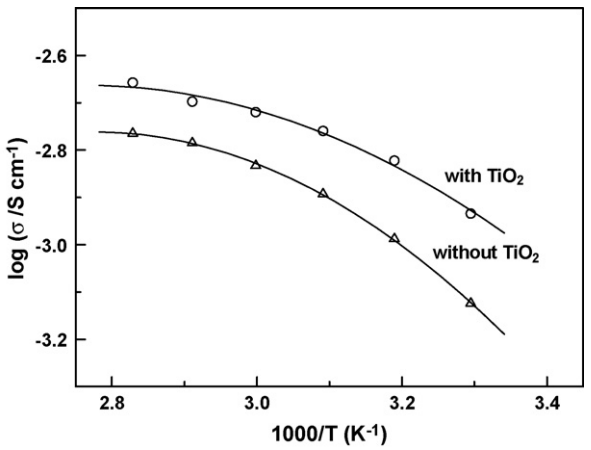

Fig. 5. Temperature dependence of ionic conductivity on the PVDF-HFP-based polymer electrolytes without and with TiO_2.

3.4. Electrochemical properties

The ionic conductivity of the polymer electrolyte membranes at room temperature was measured using the AC impedance method and the results were shown in Table 2. The ionic conductivity of PVDF-HFP electrolyte membrane with 6.5% TiO_2 was 1.66×10^{-3} S cm^{-1} at room temperature. More measurements of the ionic conductivity different temperatures were shown in Fig. 5.

As shown in Fig. 5, the conductivity was found to increase with the temperature. Both $\log\sigma$ vs. $1/T$ curves, with or without TiO_2 were nonlinear, indicating that the conductivity did not follow the

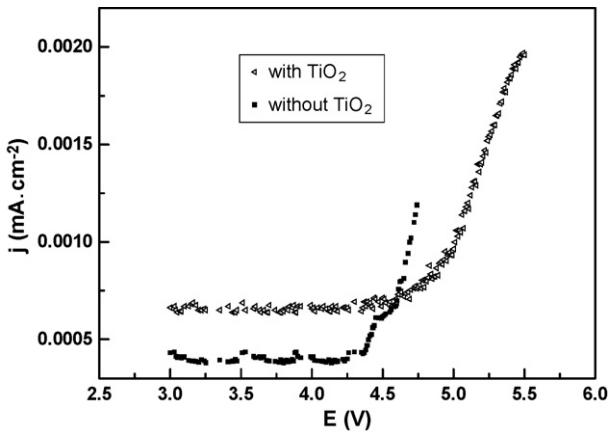

Fig. 6. Current–voltage responses of a Ni electrode in the composite electrolyte with and without TiO_2. The reference electrode was Li/Li$^+$. The scan rate was 5 mV s^{-1}.

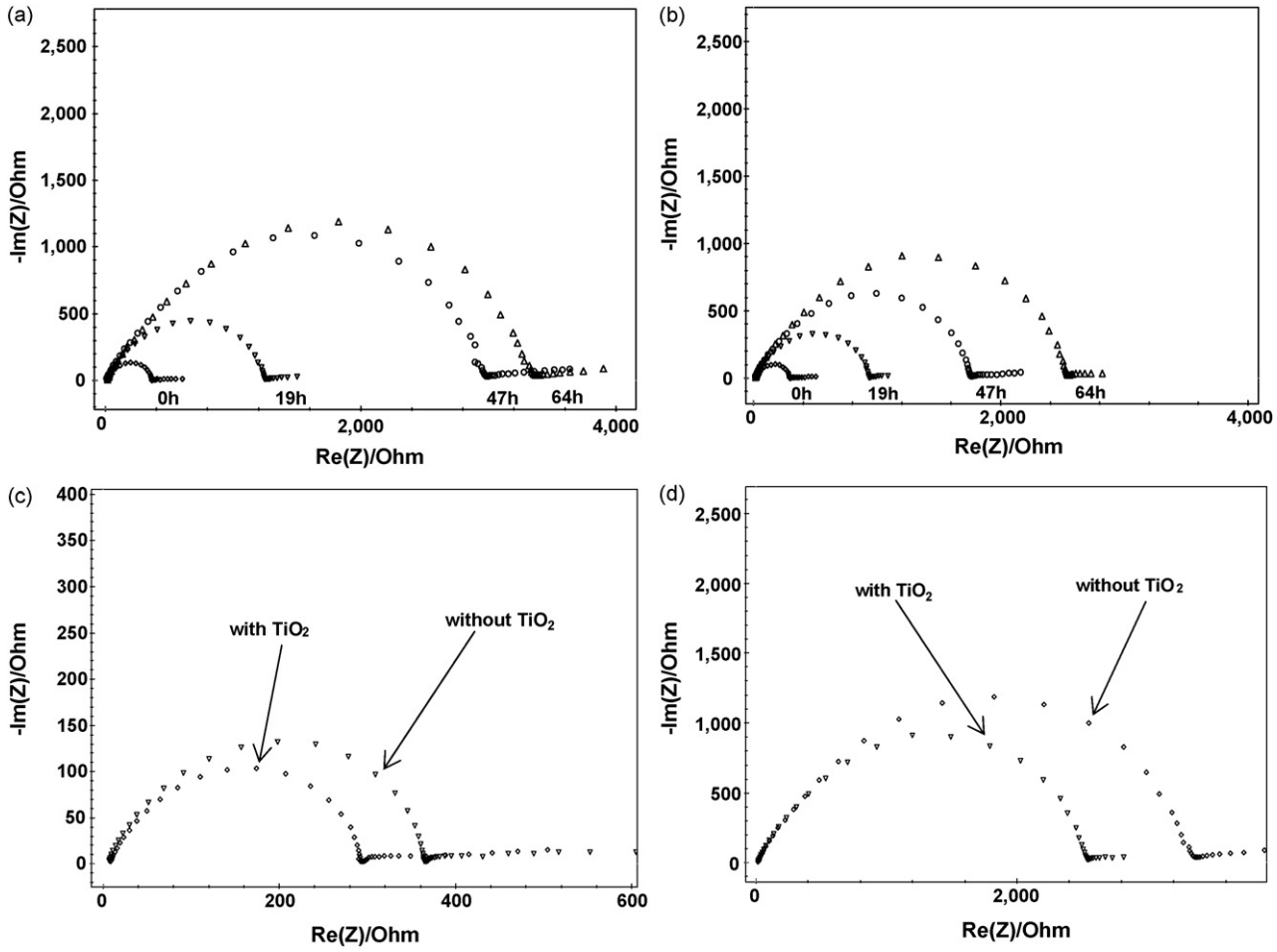

Fig. 7. Time evolution of the impedance spectra of a Li/electrolyte/Li cell stored at room temperature. (a) Electrolyte without TiO_2; (b) electrolyte with 6.5% TiO_2; (c) $t = 0$ h; (d) $t = 64$ h.

Arrhenius law but Vogel–Tammann–Fulcher (VTF) equation:

$$\sigma = AT^{-1/2} \exp\left[\frac{-E}{(T - T_0)}\right]$$

where σ is the ionic conductivity; T_0 is thought to be related to T_g, and was regressed onto the conductivity data; T is the temperature of measurement; A and E are fitting constants [24]. It is known that the porous polymer electrolyte membrane was amorphous, including several phases such as an amorphous swollen gel, crystalline strands and cavities filled with the liquid phase solution [25]. Fig. 5 shows that the conductivity difference between electrolyte membranes without TiO_2 and with TiO_2 appear to be larger at room temperature and smaller at elevated temperatures ($T = 333$ K, 60 °C). This may suggest that it is the different pseudo-activation energies that characterize the two samples, i.e. the addition of TiO_2 might restrain the growth of PVDF-HFP crystallines and result in the improvement of the uptake and the conductivity at low temperatures.

The electrochemical stability of an electrolyte is one of the essential parameters. For rechargeable lithium-ion batteries the instability in the electrolyte is known to bring out irreversible reactions and capacity fading. Fig. 6 shows a current–voltage curve of a nickel 'blocking' working electrode in a Li/composite electrolyte/Ni closed cell. It is found that the current onset occurs at around 4.7 V vs. Li/Li^+, slightly higher than the data of the electrode without TiO_2 (around 4.4 V), which means that the composite electrolyte membrane has a high anodic stability and may be used as the separator for Li-ion polymer batteries.

Besides good transport properties, compatibility with the electrode materials is another important issue to guarantee an acceptable performance in electrochemical devices. Fig. 7 shows the evolution of the impedance spectra of the Li/electrolyte membrane/Li symmetric cells with storage time at ambient temperature. The bulk resistance (R_b) of the electrolyte is the intercept on the real-axis at a high frequency, which is almost constant in the experiments. The diameter of the semicircle found in Fig. 7 corresponds to the interfacial resistance (R_i) value. From Fig. 7(a) and (b), it is seen that the total interfacial resistance (R_i) of these two kinds of electrolyte membranes increases with the increase of the storage time. The observed expansion of the impedance semicircle implies that the lithium electrode is passivated with time. Fig. 7(c) and (d) shows that R_{i2} of the composite electrolyte is less than R_{i1} of the electrolyte without TiO_2 when the storage time $t = 0$ and 64 h. It indicates that addition of TiO_2 into the polymer electrolyte has effectively reduced the rate of growth of the resistive layer on the lithium surface. The dispersion of micron TiO_2 traps impurities and prevents them from reacting at the interface [14,23]. Hence, Addition of TiO_2 to the polymer electrolyte can not only enhance the electrolyte uptake and ion conductivity of the electrolyte membrane, but also improve the interfacial capability of the electrolyte membrane/electrode interface as well as, to some degree, increase the cycle performance and rate capability of the lithium-ion battery.

Table 3
Discharge rate characteristic of a Li-ion cell with the PVDF-HFP/TiO_2 composite electrolyte

Discharge rate	Discharge current density ($mA\,g^{-1}$)	Capacity ($mAh\,g^{-1}$)
0.2 C	28	140.6
0.5 C	70	127.5
1 C	140	120.3
2 C	280	99.2

We have also investigated the rate capability of the $LiCoO_2$/composite electrolyte/Li model cell. The assembled cells were subjected to preconditioning with a cut-off voltage of 4.2 V for the upper limit and 3.0 V for the lower limit at 0.2 C rate for the first two cycles before rate capability measurements. The cell was charged up to 4.2 V at 0.2 C rate and floated at 4.2 V for 2 h before discharging. Table 3 lists the discharge rate characteristic of this cell. The discharge capacity was found to be 140.6 $mAh\,g^{-1}$ at 0.2 C; both the voltage and the capacity were found to decrease gradually with increasing the capacity rate. Even if at the high capacity rate, it still remained a better performance. At the discharge rates of 0.5, 1.0 and 2.0 C, the corresponding discharge capacities were 90.67, 85.52 and 70.53%, respectively, compared to that obtained at 0.2 C.

4. Conclusions

A porous polymer electrolyte based on PVDF-HFP for lithium-ion battery applications was prepared by the phase inversion method. The casting solution, solvent and non-solvent compositions, introduction of TiO_2 micron particles and their effects on the configuration and performance of the polymer electrolyte were investigated. The prepared electrolytes were characterized by SEM, XRD, AC impedance and charge/discharge tests. The results show that, with acetone as the solvent and de-ionized water as the non-solvent, the prepared membranes possess good pore structure and pore size for a high electrolyte uptake. When TiO_2 was added, the composite electrolyte membrane exhibits improved mechanical strength, electrolyte uptake, ionic conductivity, and the electrode/electrolyte interfacial stability. The results suggest that this porous PVDF-HFP-based composite electrolyte membrane is a potential electrolyte material for rechargeable lithium-ion batteries.

Acknowledgements

This project was funded by The National Nature Science Foundation of China (No. 50528404) and the Grant 863 Program of China (2006AA03Z224 and 2007AA05Z150).

References

[1] P.V. Wright, British Polymer Journal 7 (1975) 319.
[2] D.E. Fenton, J.M. Parker, P.V. Wright, Polymer 14 (1973) 589.
[3] F. Croce, S. Sacchetti, B. Scrosati, Journal of Power Sources 161 (2006) 560.
[4] L.R.A.K. Bandara, M.A.K.L. Dissanayake, B.E. Mellander, Electrochimica Acta 43 (1998) 1447.
[5] H.S. Kim, P. Periasamy, S.I. Moon, Journal of Power Sources 141 (2005) 293.
[6] H.S. Choe, B.G. Carroll, D.M. Pasquariello, et al., Chemistry of Materials 9 (1997) 369.
[7] A.M. Sukeshini, A. Nishimoto, M. Watanabe, Solid State Ionics 86–88 (1996) 385.
[8] S. Rajendran, M. Sivakumar, R. Subadevi, Solid State Ionics 167 (2004) 335.
[9] M. Marcinek, A. Bac, P. Lipka, et al., Journal of Physical Chemistry B 104 (2000) 11088.
[10] H.S. Kim, J.H. Shin, S.I. Moon, et al., Electrochimica Acta 48 (2003) 1573.
[11] H. Wang, H. Huang, S.L. Wunder, Journal of the Electrochemical Society 147 (2000) 2853.
[12] M.L. Yeow, L. Yutie, K. Li, Journal of Membrane Science 258 (2005) 16.
[13] W.H. Seol, Y.M. Lee, J.K. Park, Journal of Power Sources 170 (2007) 191.
[14] A. Subramania, N.T. Kalyana Sundaram, A.R. Sathiya Priya, et al., Journal of Membrane Science 294 (2007) 8.
[15] S. Suareza, S. Abbrenta, S.G. Greenbauma, et al., Solid State Ionics 166 (2004) 407.
[16] P. Johansson, P. Jacobsson, Solid State Ionics 170 (2004) 73.
[17] L. Yan, Y.S. Li, C.B. Xiang, et al., Journal of Membrane Science 276 (2006) 162.
[18] P.P. Chu, M.J. Reddy, Journal of Power Sources 115 (2003) 288.
[19] M. Kurian, M.E. Galvina, P.E. Trapa, et al., Electrochimica Acta 50 (2005) 2125.
[20] Z. Wen, Z. Gu, T. Itoh, et al., Journal of Power Sources 119–121 (2003) 427.
[21] J.Y. Xi, S.J. Miao, X.Z. Tang, Macromolecules 37 (2004) 8592.
[22] K.M. Kim, N. Park, K.S. Ryu, et al., Polymer 43 (2002) 3951.
[23] K.M. Kima, N.G. Park, K.S. Ryua, et al., Electrochimica Acta 51 (2006) 5636.
[24] Y. Aihara, S. Arai, K. Hayamizu, Electrochimica Acta 45 (2000) 1321.
[25] S.S. Zhang, K. Xu, D.L. Foster, et al., Journal of Power Sources 125 (2004) 114.